Journal of Systems Engineering and Electronics
Vol. 25, No. 3, June 2014, pp.470–482

Flocking of multi-robot systems with connectivity maintenance on directed graphs

Yutian Mao[1,2], Lihua Dou[1,2,*], Hao Fang[1,2], and Jie Chen[1,2]

1. School of Automation, Beijing Institute of Technology, Beijing 100081, China;
2. Key Laboratory of Intelligent Control and Decision of Complex Systems, Beijing 100081, China

Abstract: Analysis and design techniques for cooperative flocking of nonholonomic multi-robot systems with connectivity maintenance on directed graphs are presented. First, a set of bounded and smoothly distributed control protocols are devised via carefully designing a class of bounded artificial potential fields (APF) which could guarantee the connectivity maintenance, collision avoidance and distance stabilization simultaneously during the system evolution. The connectivity of the underlying network can be preserved, and the desired stable flocking behavior can be achieved provided that the initial communication topology is strongly connected rather than undirected or balanced, which relaxes the constraints for group topology and extends the previous work to more generalized directed graphs. Furthermore, the proposed control algorithm is extended to solve the flocking problem with a virtual leader. In this case, it is shown that all robots can asymptotically move with the desired velocity and orientation even if there is only one informed robot in the team. Finally, nontrivial simulations and experiments are conducted to verify the effectiveness of the proposed algorithm.

Keywords: multi-robot system, nonholonomic kinematics, flocking, directed network, connectivity maintenance, bounded artificial potential field (APF).

DOI: 10.1109/JSEE.2014.00054

1. Introduction

In recent years distributed flocking of autonomous agents has received considerable attention to solve a wide variety of spatially distributed tasks such as formation, surveillance, reconnaissance [1–10]. Reynolds proposed a computer animation model which consists of three heuristic rules of separation, cohesion and alignment [2]. A similar model was proposed by Vicsek et al. in [3]. Under the alignment rule, the synchronization of the headings of all agents is observed. Stimulated by [2,3], many flocking algorithms were proposed by integrating velocity consensus protocols with potential-based gradient control techniques [4–12].

It is well known that the coordination and cooperation among agents strongly rely on network connectivity. In many previous works, the underlying network is often assumed to be connected frequently enough during the system evolution to ensure reliable and efficient network-wide information exchange. However, in practice, due to limited sensing and communication capabilities of agents, for an arbitrarily given set of initial states, it is difficult or even impossible to satisfy and verify the connectivity assumption, which may result in failure of achieving the group objective. Moreover, it was also demonstrated in [13] that the network connectivity fundamentally impacts the convergence rate, the time-delay stability, and the robustness of consensus.

Motivated by the practical need to maintain network connectivity, connectivity-preserving flocking of networked multi-agent systems is rapidly becoming a hot research topic, and various strategies have been developed including both centralized [14,15] and decentralized approaches [16–28], which can be divided into three main categories: geometrical constraint technique, spectral graph theory method, and artificial potential field method. The geometrical constraint technique first appeared in [29], which was then extended to the second-order system [30]. Global connectivity can be achieved through keeping the geometric connectivity robustness of the robot networks above a certain threshold. A circum center algorithm was proposed to avoid the loss of existing connections in [31]. For the spectral graph theory method, the connecti-

Manuscript received April 16, 2013.
*Corresponding author.
This work was supported by the National Natural Science Foundation of China (61175112), the Projects of Major International (Regional) Joint Research Program (61120106010), the Foundation for Innovative Research Groups of the National Natural Science Foundation of China (G61321002), the Beijing Education Committee Cooperation Building Foundation, the Program for Changjiang Scholars and Innovative Research Team in University (IRT1208), the ChangJiang Scholars Program and the Beijing Outstanding Ph.D. Program Mentor Grant (20131000704).

vity problem can be further divided into two branches. One is to maximize the algebraic connectivity of the graph Laplacian matrix via nonconvex optimization based on subgradient or semidefinite programming (SDP) to guarantee connectivity [32]. The other is to maintain connectivity via energy functions combined with distributed eigenvalue estimators [33]. The artificial potential field (APF) method enables the system to converge to the desired configuration while preserving connectivity via superposition of the attractive and repulsive forces. The most practical way of this method is to assign each communication link an appropriate weight that is characterized as the spring force, which reaches the infinity whenever the communication link tends to break. Other solution techniques include hybrid control laws adopting market-based auctions with gossip algorithms for connectivity-preserving link additions and deletions [34,35], and topology control algorithms in Ad hoc senor networks [36], which, however, focuses more on the power consumption and routing problem than the actuation and control.

To the best of our knowledge, most of the aforementioned algorithms share the following common drawbacks.

(i) Most of the existing works on connectivity-preserving flocking problems focus on agents with purely linear integrator-type dynamics, in which it is assumed that the agent has no nonlinear kinematics or the dynamics can be fully linearized. However, mobile agents may be governed by more complicated intrinsic nonlinear dynamics in real systems [37–40]. Specifically, for industrial or military applications, when dealing with coordination and cooperation of nonholonomic wheeled mobile robots or nonholonomic robotic manipulators, the essentially nonlinear dynamics must be explicitly taken into account.

(ii) A common problem of the APF approach and the spectral graph approach is the use of unbounded potential fields to force the agents to shrink the communication links whenever they tend to leave the sensing or communication range between each other. The algorithms therein cannot guarantee connectivity maintenance whenever upper bounds on the actuation are imposed. In practical applications, however, unbounded input is impossible because real mobile agents have limited actuation capabilities, e.g., the motor cannot generate an infinitely large torque to the robots. Although in [41,42], bounded APFs are carefully designed to produce the bounded control inputs, the desired task can only be achieved for linear multi-agent systems, which limits its use in real applications.

(iii) All of the aforementioned results are restricted to undirected networks rather than directed networks. However, in many practical applications, it is natural to model the interaction topology of the heterogeneous mobile agents as a digraph for their different sensing/communication capabilities, which results in unidirectional information flow and asymmetric neighboring relationship between the interconnected agents. Moreover, the solutions for the undirected graphs can not be used for digraphs due to the symmetry-breaking properties, as they heavily rely on the ability of the agents to backtrack on a traveled path.

To overcome these drawbacks, the focus of this paper is to consider distributed flocking of multiple wheeled mobile robots with connectivity maintenance and bounded control inputs on directed graphs. The main contribution is to devise a set of bounded and smoothly distributed control protocols for agents subjected to nonhonolomic constraints. Particularly, a novel bounded and smooth APF is carefully constructed by integrating connectivity maintenance, collision avoidance and obstacle avoidance, simultaneously. Our proposed time-varying smooth controller is able to overcome the drawback of chattering by the high frequency of switching typically in discontinuous time-variant control signals in [42]. Moreover, rather than requiring the communication topology to be strongly connected and balanced [7, 22], the convergence of the group flocking behavior can still be guaranteed even if the underlying network is only strongly connected under the proposed theoretic framework, which is suitable for more general directed communication topology in real applications.

The remainder of the paper is organized as follows: Section 2 provides the background and the problem formulation. Section 3 presents the bounded flocking control laws with connectivity maintenance for nonholonomic mobile robots. The stability analysis of flocking for the overall closed-loop system is given in Section 4. Nontrivial simulations and experiments are performed in Section 5. Finally, concluding remarks and future directions are given in Section 6.

2. Preliminaries

2.1 Algebraic graph theory

Some of the main notions in the algebraic graph theory which are used in this paper are summarized [43]. Given N mobile robots, the communication topology can be modeled as a weighted directed graph $G = \{V, E\}$, where V is the finite nonempty set of all robots; $E \subseteq V \times V$ is the set of communication links among all robots. An edge (i, j) is graphically denoted by an arrow with head node i and tail node j, which implies the information flows from node j to node i. Without loss of generality, self-edges (i, i) are not allowed unless otherwise indicated. Node j is called a neighbor of node i if $(i, j) \in E$. The set of neighbors of node i is denoted as $N_i = \{j|(i, j) \in E\}$. Define the proximity-limited communication by the weighted adjacency matrix $\boldsymbol{A} \in \mathbf{R}^{N\times N}$ with the element $a_{ij} > 0$ if $j \notin N_i$.

Define the in-degree matrix of the graph as $\boldsymbol{D}^{\text{in}} = \text{diag}\{d_i^{\text{in}}\}$ with $d_i^{\text{in}} = \sum_{j=1}^{N} a_{ij}$ as the diagonal elements. The Laplacian matrix of G is then given by $\boldsymbol{L} = \boldsymbol{D}^{\text{in}} - \boldsymbol{A}$ which is positive and semi-definite for undirected graphs. $\boldsymbol{L}\mathbf{1}_N = \mathbf{0}$, where $\mathbf{1}_N$ is the N-dimensional column vector of all ones. Accordingly, define the out-degree of node i as $d_i^{\text{out}} = \sum_{j=1}^{N} a_{ji}$ and the out-degree matrix as $\boldsymbol{D}_{\text{out}} = \text{diag}\{d_i^{\text{out}}\}$. The node i is balanced if its in-degree equals its out-degree, i.e., $\sum_{j=1}^{N} a_{ji} = \sum_{j=1}^{N} a_{ij}$. A directed graph is balanced if all of its nodes are balanced. Then, for an undirected graph, all undirected graphs are balanced.

In a directed graph, a sequence of successive edges in the form $\{(i, l), (l, m), \ldots, (k, j)\}$ is a directed path from node i to node j. A digraph is said to have a spanning tree, if there is a node r (called the root) from which there is a directed path to any other node in the graph. And a digraph is said to be strongly connected, if there is a directed path from node i to node j for all distinct nodes i and j. In particular, $N(\boldsymbol{L}) = \text{span}\{\mathbf{1}_N\}$ if and only if the graph contains a spanning tree, where $N(\cdot)$ is the kernel space, $\text{span}\{\cdot\}$ denotes the spanning space.

Lemma 1 [44] Let the directed graph G be strongly connected. Then there exists a positive vector $\boldsymbol{y} > \mathbf{0}$, which is the left eigenvector of $\boldsymbol{L}(G)$ associated with the eigenvalue $\lambda = 0$, i.e., $\boldsymbol{L}(G)\mathbf{1}_N = \mathbf{0}$ and $\boldsymbol{y}^{\mathrm{T}}\mathbf{1}_N = \mathbf{1}$.

2.2 Problem statement

Consider a group of N wheeled mobile robots moving on the Euclidean plane with the dynamics described by the following nonholonomic differential equations

$$\begin{cases} \dot{x}_i = \boldsymbol{v}_i \cos\theta_i \\ \dot{y}_i = \boldsymbol{v}_i \sin\theta_i \\ \dot{\theta}_i = \boldsymbol{\omega}_i \\ \dot{\boldsymbol{v}}_i = \boldsymbol{a}_i \\ i = 1, 2, \ldots, N \end{cases} \tag{1}$$

where $\boldsymbol{r}_i = (x_i, y_i)^{\mathrm{T}} \in \mathbf{R}^2$ is the position vector of robot i, $\boldsymbol{v}_i \in \mathbf{R}^2$ is the linear velocity of agent i, $\theta_i \in \mathbf{R}$ is the orientation of agent i, and $\boldsymbol{a}_i, \boldsymbol{\omega}_i$ are linear acceleration and angular velocity vectors respectively, which are also control inputs acting on agent i. Furthermore, denote $\boldsymbol{r} = (\boldsymbol{r}_1^{\mathrm{T}}, \ldots, \boldsymbol{r}_N^{\mathrm{T}})^{\mathrm{T}}, \boldsymbol{v} = (\boldsymbol{v}_1^{\mathrm{T}}, \ldots, \boldsymbol{v}_N^{\mathrm{T}})^{\mathrm{T}}$ and $\boldsymbol{\theta} = (\theta_1, \ldots, \theta_N)^{\mathrm{T}}$ as the stack position, velocity and orientation vectors of the system, respectively. Let $\boldsymbol{r}_{ij} = \boldsymbol{r}_i - \boldsymbol{r}_j$ be the relative position vector between robots i and j.

The control objective here is to derive a set of bounded distributed controllers using only local information to steer all the robots with nonholonomic kinematics (1) to achieve velocity consensus, collision avoidance with each other, and finally move coherently in a common orientation, while guaranteeing that the underlying graph is strongly connected as the system evolves, provided that the given graph is initially strongly connected but not balanced.

3. Control development

3.1 Flocking without virtual leader

Lemma 2 [45] Suppose that the eigenvalues of symmetric matrices $\boldsymbol{A}, \boldsymbol{B} \in \mathbf{R}^{N\times N}$ satisfy $\lambda_1(\boldsymbol{A}) \leqslant \cdots \leqslant \lambda_N(\boldsymbol{A})$ and $\lambda_1(\boldsymbol{B}) \leqslant \cdots \leqslant \lambda_N(\boldsymbol{B})$. Then the following inequality holds:

$$\lambda_{i+j-1}(\boldsymbol{A} + \boldsymbol{B}) \geqslant \lambda_i(\boldsymbol{A}) + \lambda_j(\boldsymbol{B}) \tag{2}$$

where $i + j \leqslant N + 1, 1 \leqslant i, j \leqslant N$.

Lemma 3 Suppose that the directed graph is strongly connected. Define

$$\begin{cases} \boldsymbol{P} = \text{diag}\{p_i\} \in \mathbf{R}^{N\times N} \\ \boldsymbol{Q} = \boldsymbol{PL} + \boldsymbol{L}^{\mathrm{T}}\boldsymbol{P} \end{cases} \tag{3}$$

where $\boldsymbol{P} = [p_1, p_2, \ldots, p_N]^{\mathrm{T}}$ is the positive left eigenvector of $\boldsymbol{L}$ as defined in Lemma 1. Then $\boldsymbol{P} > \mathbf{0}, \boldsymbol{Q} \geqslant \mathbf{0}$.

Proof It is straightforward to begin with

$$\boldsymbol{x}^{\mathrm{T}}\boldsymbol{PLx} = \sum_{i=1}^{N} p_i x_i \sum_{i=1}^{N} a_{ij}(x_i - x_j).$$

Since $\boldsymbol{L}^{\mathrm{T}}\boldsymbol{p} = \mathbf{0}$ implies $p_i \sum_{j=1}^{N} a_{ij} = \sum_{j=1}^{N} p_j a_{ji}$, we have

$$\sum_{i=1}^{N} p_i x_i \sum_{j=1}^{N} a_{ij}(x_i - x_j) =$$

$$\sum_{i=1}^{N} x_i^2 \sum_{j=1}^{N} p_j a_{ji} - \sum_{i=1}^{N} p_i \sum_{j=1}^{N} a_{ij} x_i x_j =$$

$$\sum_{i=1}^{N} x_j^2 \sum_{j=1}^{N} p_i a_{ij} - \sum_{i=1}^{N} \sum_{j=1}^{N} p_i a_{ij} x_i x_j =$$

$$\sum_{i=1}^{N} p_i \sum_{j=1}^{N} a_{ij} x_j (x_j - x_i).$$

Then it follows that

$$\begin{aligned}&\boldsymbol{x}^{\mathrm{T}}\boldsymbol{Q}\boldsymbol{x}=2\boldsymbol{x}^{\mathrm{T}}\boldsymbol{P}\boldsymbol{L}\boldsymbol{x}=\\&2\sum_{i=1}^{N}p_ix_i\sum_{j=1}^{N}a_{ij}(x_i-x_j)=\\&\sum_{i=1}^{N}p_ix_i\sum_{j=1}^{N}a_{ij}(x_i-x_j)+\\&\sum_{i=1}^{N}p_ix_j\sum_{j=1}^{N}a_{ij}(x_j-x_i)=\\&\sum_{i=1}^{N}p_i\sum_{j=1}^{N}a_{ij}(x_i-x_j)^2\geqslant 0\end{aligned}$$

□

Lemma 4 Let the digraph be strongly connected, and $\boldsymbol{Q}$ is defined in (3), then $N(\boldsymbol{Q})=N(\boldsymbol{L})=\mathrm{span}\{\boldsymbol{1}_N\}$.

Proof First, it is obvious that $N(\boldsymbol{L})\subseteq N(\boldsymbol{Q})$ according to (3). Since the directed graph is strongly connected, $N(\boldsymbol{L})=\mathrm{span}\{\boldsymbol{1}_N\}, \mathrm{span}\{\boldsymbol{1}_N\}\subseteq N(\boldsymbol{Q})$. Therefore, $\boldsymbol{Q}\boldsymbol{1}_N=\boldsymbol{0}$ and $\boldsymbol{Q}$ is a valid symmetric Laplacian matrix of an augmented graph $\bar{G}$, which has the same node set as graph $\bar{G}$, and the weight of edge (i,j) is $\bar{a}_{ij}=p_ia_{ij}+p_ja_{ji}$. It is obvious that $\bar{G}$ is undirected and hence balanced. We hereafter call $\bar{G}$ as the weighted mirror graph of the original digraph G.

Next, we need to show that the rank of $\boldsymbol{Q}$ is $N-1$. Since $p_i>0$, it is clear that if $a_{ij}>0$, then $\bar{a}_{ij}>0$. Strong connectedness of graph G implies the strong connectedness of the corresponding weighted mirror graph G, thus we have $N(\boldsymbol{Q})=\mathrm{span}\{\boldsymbol{1}_N\}$ and $N(\boldsymbol{Q})=N(\boldsymbol{L})$. □

Let $\varepsilon_2\in\bigcap_{j=1}^{N}(0,R_j)$ be a small hysteresis constant, where R_j is the communication radius of agent j. Link additions and deletions are regulated by the following rules:

(i) Initial links are generated by $E(0)=\{(i,j)|||\boldsymbol{r}_{ij}(0)||<R_j-\varepsilon_0\}$, where $0<\varepsilon_0<\varepsilon_2$.

(ii) If $(i,j)\notin E(t^-)\wedge||\boldsymbol{r}_{ij}(t)||<R_j-\varepsilon_2$, then (i,j) is a new link being added to $E(t)$.

(iii) If $(i,j)\in E(t^-)\wedge||\boldsymbol{r}_{ij}(t)||\geqslant R_j$, then $(i,j)\notin E(t)$.

t^- refers to the time instant before topology changes; $\wedge$ is the boolean AND operation.

In order to realize the desired stable flocking behavior, the control protocols should contain two components. One is responsible for synchronizing the headings and the linear velocities of all robots, and the other one aims at steering them to move cohesively without collisions while guaranteeing strong connectedness of the entire system as time evolves. For this end, the explicitly distributed flocking control protocol for each robot i is designed as follows:

$$\begin{cases}\boldsymbol{a}_i=-\sum\limits_{j\in N_i}a_{ij}(\langle\nabla_{\boldsymbol{r}_i}V_i,(\cos\theta_i,\sin\theta_i)^{\mathrm{T}}\rangle-\\\quad\langle\nabla_{\boldsymbol{r}_j}V_j,(\cos\theta_j,\sin\theta_j)^{\mathrm{T}}\rangle)\left\|\sum\limits_{j\in N_i}a_{ij}(\boldsymbol{v}_i-\boldsymbol{v}_j)\right\|-\\\quad\dfrac{1}{2}\nabla_{\boldsymbol{r}_i}V_i-k\sum\limits_{j\in N_i}a_{ij}(\boldsymbol{v}_i-\boldsymbol{v}_j)\\\omega_i=-\sum\limits_{j\in N_i}a_{ij}(\langle\nabla_{\boldsymbol{r}_i}V_i,(-\sin\theta_i,\cos\theta_i)^{\mathrm{T}}\rangle-\\\quad\langle\nabla_{\boldsymbol{r}_j}V_j,(-\sin\theta_j,\cos\theta_j)^{\mathrm{T}}\rangle)\left\|\sum\limits_{j\in N_i}a_{ij}(\theta_i-\theta_j)\right\|-\\\quad k\sum\limits_{j\in N_i}a_{ij}(\theta_i-\theta_j)\end{cases}\tag{4}$$

where $k>0$ is the control gain; $\langle\cdot\rangle$ denotes the inner product of the vectors; $|\cdot|$ is defined componenwise; $V_i=\sum_{j\in N_i}V_{ij}$ is the potential defined as the sum of all artificial potentials associated with each of its neighbors; $\langle\nabla_{\boldsymbol{r}_i}V_i,(\cos\theta_i,\sin\theta_i)^{\mathrm{T}}\rangle$ and $\langle\nabla_{\boldsymbol{r}_i}V_i,(-\sin\theta_i,\cos\theta_i)^{\mathrm{T}}\rangle$ denote the projection of $\nabla_{\boldsymbol{r}_i}V_i$ onto the directions aligned with and perpendicular to the translational velocity of each robot i, respectively.

Remark 1 Note that in (4), the first two terms of $\boldsymbol{a}_i$ are responsible for relative distance stabilization, collision avoidance as well as connectivity maintenance simultaneously, while the last term of $\boldsymbol{a}_i$ is responsible for reaching velocity consensus among all robots. Similarly, the first two terms of ω_i in (4) aim at synchronizing the headings of all neighboring robots. The combination of $\boldsymbol{a}_i$ and ω_i constitutes the flocking control input for each robot i, and the boundedness of (4) is strongly dependent on the design of the finite potentials $V_{ij}(\forall j\in N_i)$, which will be detailed later.

To enable the overall system to achieve the desired stable flocking motion using only bounded control inputs, $V_{ij}(\|\boldsymbol{r}_{ij}\|)$ should be carefully designed to be a kind of bounded and nonnegative artificial potential with respect to $\boldsymbol{r}_{ij}$ while integrating connectivity maintenance and collision avoidance, such that

(i) $V_{ij}(\|\boldsymbol{r}_{ij}\|)$ is continuously differentiable for $\|\boldsymbol{r}_{ij}\|\in(0,R_j)$;

(ii) $V_{ij}(\|\boldsymbol{r}_{ij}\|)$ is monotonically decreasing for $\|\boldsymbol{r}_{ij}\|\in(0,d)$ and monotonically increasing for $\|\boldsymbol{r}_{ij}\|\in(d,R_j)$, where $0<\varepsilon_1<d<R_j-\varepsilon_2$;

(iii) $V_{ij}(0)=c_1+H_{\max}$, $V_{ij}(R_j)=c_2+H_{\max}$, where $c_1,c_2\geqslant 0$, $H_{\max}=\boldsymbol{v}(0)^{\mathrm{T}}\boldsymbol{P}\boldsymbol{v}(0)+\boldsymbol{\theta}(0)^{\mathrm{T}}\boldsymbol{P}\boldsymbol{\theta}(0)+N(N-1)V_{\max}$, $V_{\max}=\max\{V(\varepsilon_1),V(R_{\max}-\varepsilon_2)\}$, $R_{\max}=\max\limits_{i\in V}\{R_i\}$ and $\varepsilon_1=\min\limits_{i,j\in V}\{\|\boldsymbol{r}_{ij}(0)\|$.

Condition (i) aims at producing a smooth controller for each robot; condition (ii) illustrates that the potential V_{ij} provides an attractive or repulsive force between agents i and j when their distance tends to R_j or zero; condition (iii) states that the potential will be sufficiently large when the distance between them reaches R_j or zero, which guarantees the connectivity maintenance and collision avoidance. One candidate example is given as below:

$$V(||\boldsymbol{r}_{ij}||)=\frac{(||\boldsymbol{r}_{ij}||-d)^2(R_j-||\boldsymbol{r}_{ij}||)}{||\boldsymbol{r}_{ij}||+\dfrac{d^2(R_j-||\boldsymbol{r}_{ij}||)}{c_1+H_{\max}}}+$$

$$\frac{||\boldsymbol{r}_{ij}||(||\boldsymbol{r}_{ij}||-d)^2}{(R_j-||\boldsymbol{r}_{ij}||)+\dfrac{||\boldsymbol{r}_{ij}||(R_j-d)^2}{c_2+H_{\max}}}. \quad (5)$$

Note that in [18,20,23], two kinds of specific potential functions are introduced and tend to the infinity when the relative distance between two agents i and j tends to R, which may not be practical since it will require infinitely large (unbounded) control effort. Let $f_{\max}$ be the magnitude of the maximum potential force, then we have the following theorem.

Theorem 1 Consider a system of N mobile robots with nonholonomic dynamics (1), each steered by protocol (4). Suppose that the initial energy $H(0)$ is finite and the initial communication network $G(0)$ is strongly connected but not balanced, and

$$\lambda_2(\boldsymbol{Q}(0))>2f_{\max}N^2(N-1)/k$$

where $\boldsymbol{Q}=\boldsymbol{PL}+\boldsymbol{L}^{\mathrm{T}}\boldsymbol{P}$.

Then the network will be strongly connected for all time, all the agents asymptotically converge to the same velocity, collisions between agents are avoided and all the interagent distances are stabilized.

Proof Consider the positive semi-definite function as

$$H=\sum_{i=1}^{N}p_i\sum_{j\in N_i}V_{ij}(\|\boldsymbol{r}_{ij}\|)+\boldsymbol{v}^{\mathrm{T}}\boldsymbol{Pv}+\boldsymbol{\theta}^{\mathrm{T}}\boldsymbol{P\theta}.$$

Assume that $G(t)$ switches at time t_k $(k=1,2,\dots)$ and keeps fixed over each time interval $[t_{k-1},t_k)$. Specifically, $H(0)$ is finite, then take the time derivative of $H(t)$ on $[0,t_1)$, which yields

$$\dot{H}=\sum_{i=1}^{N}\boldsymbol{v}_i^{\mathrm{T}}\dot{p}_i\sum_{j\in N_i(t)}\nabla_{\boldsymbol{r}_i}V_{ij}+2\boldsymbol{\theta}^{\mathrm{T}}\boldsymbol{P}\cdot$$
$$(-\boldsymbol{kL\theta}-\boldsymbol{L}(\nabla\boldsymbol{V})_{\perp}||\boldsymbol{L\theta}||)+$$
$$2\boldsymbol{v}^{\mathrm{T}}\boldsymbol{P}\left(-k\boldsymbol{Lv}-\boldsymbol{L}(\nabla\boldsymbol{V})_{\|}||\boldsymbol{Lv}||-\frac{1}{2}\nabla\boldsymbol{V}\right)=$$
$$k\boldsymbol{\theta}^{\mathrm{T}}(\boldsymbol{PL}+\boldsymbol{L}^{\mathrm{T}}\boldsymbol{P})\boldsymbol{\theta}-2\boldsymbol{\theta}^{\mathrm{T}}\boldsymbol{PL}(\nabla\boldsymbol{V})_{\perp}||\boldsymbol{L\theta}||-$$
$$k\boldsymbol{v}^{\mathrm{T}}(\boldsymbol{PL}+\boldsymbol{L}^{\mathrm{T}}\boldsymbol{P})\boldsymbol{v}-2\boldsymbol{v}^{\mathrm{T}}\boldsymbol{PL}(\nabla\boldsymbol{V})_{\|}||\boldsymbol{Lv}|| \quad (6)$$

where $\nabla\boldsymbol{V}=[\nabla_{\boldsymbol{r}_1}V_1,\nabla_{\boldsymbol{r}_2}V_2,\dots,\nabla_{\boldsymbol{r}_N}V_N]^{\mathrm{T}}$; $(\nabla\boldsymbol{V})_{\perp}=[(\nabla_{\boldsymbol{r}_1}V_1)_{\perp},\dots,(\nabla_{\boldsymbol{r}_N}V_N)_{\perp}]^{\mathrm{T}}$; $(\nabla\boldsymbol{V})_{\|}=[(\nabla_{\boldsymbol{r}_1}V_1)_{\|},\dots,(\nabla_{\boldsymbol{r}_N}V_N)_{\|}]^{\mathrm{T}}$; $(\nabla_{\boldsymbol{r}_i}V_i)_{\|}$ and $(\nabla_{\boldsymbol{r}_i}V_i)_{\perp}$ are the components of $\nabla_{\boldsymbol{r}_i}V_i$ when expressed in a body-fixed coordinate frame, aligned with and perpendicular to the translational velocity of robot i, respectively.

Further, decompose $\boldsymbol{v}$ and $\boldsymbol{\theta}$ as $\boldsymbol{v}=\boldsymbol{v}^{\boldsymbol{1}_N}\oplus\boldsymbol{v}^{\boldsymbol{1}_N^{\perp}}$ and $\boldsymbol{\theta}=\boldsymbol{\theta}^{\boldsymbol{1}_N}\oplus\boldsymbol{\theta}^{\boldsymbol{1}_N^{\perp}}$. Superscripts $\boldsymbol{1}_N$ and $\boldsymbol{1}_N^{\perp}$ denote the components along the direction of the vector of all ones and its orthogonal. Then, (6) becomes

$$\dot{H}=-k\boldsymbol{\theta}^{\mathrm{T}}(\boldsymbol{PL}+\boldsymbol{L}^{\mathrm{T}}\boldsymbol{P})\boldsymbol{\theta}-2\boldsymbol{\theta}^{\mathrm{T}}\boldsymbol{PL}(\nabla\boldsymbol{V})_{\perp}||\boldsymbol{L\theta}||-$$
$$k\boldsymbol{v}^{\mathrm{T}}(\boldsymbol{PL}+\boldsymbol{L}^{\mathrm{T}}\boldsymbol{P})\boldsymbol{v}-2\boldsymbol{v}^{\mathrm{T}}\boldsymbol{PL}(\nabla\boldsymbol{V})_{\|}||\boldsymbol{Lv}||\leqslant$$
$$-k\lambda_2(\boldsymbol{Q})||\boldsymbol{\theta}^{\boldsymbol{1}_N^{\perp}}||^2+2f_{\max}||\boldsymbol{\theta}^{\boldsymbol{1}_N^{\perp}}||\left\|L\boldsymbol{\theta}^{1_N^{\perp}}\right\|-$$
$$k\lambda_2(\boldsymbol{Q})||\boldsymbol{v}^{\boldsymbol{1}_N^{\perp}}||^2+2f_{\max}||\boldsymbol{v}^{\boldsymbol{1}^{\perp}}||\left\|\boldsymbol{Lv}^{\boldsymbol{1}_N^{\perp}}\right\|\leqslant$$
$$-(k\lambda_2(\boldsymbol{Q})-2f_{\max}N^2(N-1))||\boldsymbol{\theta}^{\boldsymbol{1}_N^{\perp}}||^2-$$
$$(k\lambda_2(\boldsymbol{Q})-2f_{\max}N^2(N-1))||\boldsymbol{v}^{\boldsymbol{1}_N^{\perp}}||^2. \quad (7)$$

According to the initial condition $\lambda_2(\boldsymbol{Q}(0))>2f_{\max}N^2(N-1)/k$, we have

$$\dot{H}(t)\leqslant 0,\quad \forall t\in[0,t_1). \quad (8)$$

Therefore, $H(t)$ will be decreasing in $[0,t_1)$, and from (5), one has $V_{ij}(R_j)\geqslant H_{\max}>H(0)$ $(\forall(i,j)\in E)$. Therefore, for each robot i, no edge-distance will tend to R_j $(\forall j\in N_i)$. Hence, new edges must be added into the network at the switching time t_1 and the strong connectedness of $G(t)$ is preserved for $t\in[0,t_1)$. Without loss of generality, assume that there are N_1 new links being added to the communication network at time t_1. According to the fact that $G(t)$ is strongly connected over $t\in[0,t_1)$, one has that $G(t)$ contains at least N edges, thus it follows $0<N_1\leqslant N_{\max}=N(N-2)$, and $H(t_1)<H(0)+N_{\max}V(\|R_{\max}-\varepsilon_2\|)$. Furthermore, according to the fact that new edges must be added into the network at the switching time and applying Lemma 2 to the undirected weighted mirror graph $\bar{G}$, we have $\lambda_2(\boldsymbol{Q}(t_1))\geqslant\lambda_2(\boldsymbol{Q}(0))$. Therefore, for arbitrary $k\geqslant 2$, one may get $\lambda_2(\boldsymbol{Q}(t_{k-1}))>\lambda_2(\boldsymbol{Q}(0))$ by induction. Following the same analysis and taking the time derivative of $H(t)$ in $[t_{k-1},t_k)$, we can get

$$\dot{H}(t)\leqslant-(k\lambda_2(\boldsymbol{Q}(t_{k-1}))-2f_{\max}N^2(N-1))||\boldsymbol{\theta}^{\boldsymbol{1}_N^{\perp}}||^2-$$
$$(k\lambda_2(\boldsymbol{Q}(t_{k-1}))-2f_{\max}N^2(N-1))||\boldsymbol{v}^{\boldsymbol{1}_N^{\perp}}||^2 \quad (9)$$

which implies

$$H(t)\leqslant H(t_{k-1})<H_{\max},\quad \forall t\in[t_{k-1},t_k);k=1,2,\dots \quad (10)$$

Thus, no edge-distance will be tend to R_j $(\forall j \in N_i)$, which implies that no edges will be lost at time t_k. Since $G(0)$ is strongly connected and no edges in $E(0)$ will be lost. $G(t)$ will be strongly connected for all time. Assume that there are N_k new links being added to the interaction network at time t_k. Clearly, $0 < N_k \leqslant N_{\max}$, then we have

$$H(t_k) \leqslant H(0) + (N_1 + N_2 + \ldots + N_k) \leqslant H_{\max}. \quad (11)$$

Since there are at most $N_{\max}$ new edges that can be added to $G(t)$, one has $k \leqslant N_{\max}$ $(\forall t \geqslant 0)$. Therefore, the number of switching times k is finite, which implies that the interaction topology $G(t)$ eventually becomes fixed. Hence, the rest analysis can be restricted to $[t_k, +\infty)$. Note that the length of each edge will not be longer than $\max\{V^{-1}(H_{\max})\}$ and not be shorter than $\min\{V^{-1}(H_{\max})\}$ during the system evolution. Hence, the set $\Omega = \{\bar{\boldsymbol{r}} \in D, \boldsymbol{\theta} \in \mathbf{R}^N, \boldsymbol{v} \in \mathbf{R}^{2N} | H(\bar{\boldsymbol{r}}, \boldsymbol{\theta}, \boldsymbol{v}) \leqslant H_{\max}\}$ is a positively invariant set, where $D = \{\bar{\boldsymbol{r}} \in \mathbf{R}^{2N^2} | \boldsymbol{r}_{ij} \in [\min\{V^{-1}(H_{\max})\}, \max\{V^{-1}(H_{\max})\}], \forall (i,j) \in E(t)\}$ and $\bar{\boldsymbol{r}} = (\boldsymbol{r}_{11}^{\mathrm{T}}, \ldots, \boldsymbol{r}_{1N}^{\mathrm{T}}, \ldots, \boldsymbol{r}_{N1}^{\mathrm{T}}, \ldots, \boldsymbol{r}_{NN}^{\mathrm{T}})^{\mathrm{T}}$. Because $G(t)$ is strongly connected for all time, $\|\boldsymbol{r}_{ij}\| \leqslant (N-1)R_{\max}, \forall (i,j) \in E(t)$. Since $H(t) \leqslant H(0) \leqslant H_{\max}$, then it follows $||\boldsymbol{v}_i|| \leqslant \sqrt{2H_{\max}}, |\theta_i| \leqslant \sqrt{2H_{\max}}$. Therefore, Ω is compact. Note that system (1) with control input (2) is an autonomous system, at least in the concerned time interval $[t_k, \infty)$. Then the LaSalle's invariance principle can be applied to infer that, if the initial conditions of the system lies in Ω [46], all the trajectories will converge to the largest invariant set inside the region

$$S = \{\tilde{\boldsymbol{r}} \in D, \boldsymbol{\theta} \in \mathbf{R}^N, \boldsymbol{v} \in \mathbf{R}^{2N} | \dot{H} = 0\}. \quad (12)$$

From (9), $\dot{H} = 0$ if and only if $\boldsymbol{\theta}^{\mathbf{1}_N^{\perp}} = \mathbf{0}$ and $\boldsymbol{v}^{\mathbf{1}_N^{\perp}} = \mathbf{0}$, which implies that $\boldsymbol{v}$ and $\boldsymbol{\theta}$ are parallel to $\mathbf{1}_N$, i.e., $\theta_1 = \cdots = \theta_N = \theta^\star, \boldsymbol{v}_1 = \cdots = \boldsymbol{v}_N = \boldsymbol{v}^\star$. This means that all the robots asymptotically move with the same velocity and the same orientation. Then we have

$$\boldsymbol{\omega}_1 = \cdots = \boldsymbol{\omega}_N = \mathbf{0}, \quad \boldsymbol{a}_1 = \cdots = \boldsymbol{a}_N = \mathbf{0}.$$

Subtituting (4) into (1), then in the steady state, we have

$$\dot{x}_i = \boldsymbol{v}^\star \cos\theta^\star, \quad \dot{y}_i = \boldsymbol{v}^\star \sin\theta^\star \quad (13)$$

and

$$\boldsymbol{a} = -\begin{bmatrix} \nabla_{\boldsymbol{r}_1} V_{1j} \\ \vdots \\ \nabla_{\boldsymbol{r}_N} V_{Nj} \end{bmatrix} = \mathbf{0} \quad (14)$$

where $\boldsymbol{a} = [\boldsymbol{a}_1^{\mathrm{T}}, \boldsymbol{a}_2^{\mathrm{T}}, \ldots, \boldsymbol{a}_N^{\mathrm{T}}]^{\mathrm{T}} \in \mathbf{R}^{2N}$. Equation (14) implies that the multi-robot systems asymptotically converge to a fixed configuration corresponding to an extremum of robot's global potential. However, every point but local minima is an unstable equilibrium, thus almost every final configuration locally minimizes the global potential $\sum_{j\in N_i} \nabla_{\boldsymbol{r}_i} V_{ij}$ associated with each robot i.

Finally, suppose that robots i and j collide with each other. However, in view of (11), we have $H(t) \leqslant H_{\max}$ $(\forall t \geqslant 0)$, and from (5), we have $\lim_{\|\boldsymbol{r}_{ij}\| \to 0} V_{ij}(0) \geqslant H_{\max}$, which reaches a confliction. Therefore, collisions among agents are avoided. □

3.2 Flocking with a virtual leader

In this section, the problem of flocking control with a virtual leader is investigated. Denote $\boldsymbol{r}_l = [x_l, y_l]^{\mathrm{T}}$, $\boldsymbol{v}_l$ and θ_l are the position, constant velocity and orientation vectors of the virtual leader. Then denote $\tilde{\boldsymbol{r}}_i = \boldsymbol{r}_i - \boldsymbol{r}_l$, $\tilde{\boldsymbol{v}}_i = \boldsymbol{v}_i - \boldsymbol{v}_l$ and $\tilde{\theta}_i = \theta_i - \theta_l$ as the position error, velocity error and orientation error vectors, respectively. By the definition of $V_{ij}(\|\boldsymbol{r}_{ij}\|)$, it follows that $V_{ij}(\|\boldsymbol{r}_{ij}\|) = \tilde{V}_{ij}(\|\tilde{\boldsymbol{r}}_{ij}\|)$, where $\tilde{\boldsymbol{r}}_{ij} = \tilde{\boldsymbol{r}}_i - \tilde{\boldsymbol{r}}_j$. Here, it is assumed that only a small fraction $\delta \in [0, 1)$ of the robots can communicate with the leader and gets its information. In this case, similar to the design idea of (4), the explicit form of the tracking control protocol for each follower i is specified as follows:

$$\begin{cases} \boldsymbol{a}_i = -\langle \nabla_{\tilde{\boldsymbol{r}}_i} \tilde{V}_i, (\cos\theta_i, \sin\theta_i)^{\mathrm{T}} \rangle | \sum_{j\in N_i} a_{ij}(\boldsymbol{v}_i - \boldsymbol{v}_j)| - \\ \qquad \frac{1}{2} \sum_{j\in N_i \cup \{l\}} \nabla_{\tilde{\boldsymbol{r}}_i} \tilde{V}_{ij}(||\tilde{\boldsymbol{r}}_{ij}||) - k \sum_{j\in N_i} a_{ij}(\boldsymbol{v}_i - \boldsymbol{v}_j) - h_i \tilde{\boldsymbol{v}}_i \\ \omega_i = -\langle \nabla_{\tilde{\boldsymbol{r}}_i} \tilde{V}_i, (-\sin\theta_i, \cos\theta_i)^{\mathrm{T}} \rangle | \sum_{j\in N_i} a_{ij}(\theta_i - \theta_j)| - \\ \qquad k \sum_{j\in N_i} a_{ij}(\theta_i - \theta_j) - h_i \tilde{\theta}_i \end{cases} \quad (15)$$

where $\tilde{V}_i = \sum_{j\in N_i} \tilde{V}_{ij}$; $|\cdot|$ is the absolute value operator acting on each component of a vector; if robot i is the informed robot, $h_i = 1$, otherwise, $h_i = 0$.

Remark 2 Note that in (15), the first two terms of $\boldsymbol{a}_i$ are responsible for relative distance stabilization, collision avoidance as well as connectivity maintenance simultaneously, while the last two terms of $\boldsymbol{a}_i$ are responsible for achieving velocity consensus among all followers and the virtual leader. Similarly, ω_i aims at synchronizing the orientations among all followers with the virtual leader. Both $\boldsymbol{a}_i$ and ω_i constitute the final tracking control inputs for each follower i.

Then we have the theoretical result which is stated as the following theorem.

Theorem 2 Consider a system of N mobile robots with dynamics (1), each of them is steered by the control protocol (15). Suppose that the initial network $G(0)$ is strongly connected and the initial energy is finite. If

$$\lambda_2((k\boldsymbol{Q}+2\boldsymbol{P}\boldsymbol{H})(0)) > \frac{2f_{\max}N(N-1)}{k} \quad (16)$$

where $\boldsymbol{H}=\operatorname{diag}\{h_1,h_2,\dots,h_N\}$. Then $G(t)$ is strongly connected for all $t \geqslant 0$, all the robots asymptotically converge to the desired velocity and orientation with the virtual leader, while collisions between all robots are avoided.

Proof Consider the following positive semi-definite Lyapunov function:

$$U=\sum_{i=1}^{N} p_i \sum_{j\in N_i\cup\{l\}} \tilde{V}_{ij}(||\tilde{\boldsymbol{r}}_{ij}||)+\tilde{\boldsymbol{v}}^{\mathrm{T}}\boldsymbol{P}\tilde{\boldsymbol{v}}+\tilde{\boldsymbol{\theta}}^{\mathrm{T}}\boldsymbol{P}\tilde{\boldsymbol{\theta}} \quad (17)$$

where $\tilde{\boldsymbol{v}}=[\tilde{\boldsymbol{v}}_1^{\mathrm{T}},\dots,\tilde{\boldsymbol{v}}_N^{\mathrm{T}}]^{\mathrm{T}}$ and $\tilde{\boldsymbol{\theta}}=[\tilde{\theta}_1,\dots,\tilde{\theta}_N]^{\mathrm{T}}$. Similar to the proof of Theorem 1, it can be shown that the time derivative of $U(t)$ in $[t_{k-1},t_k)$ is

$$\begin{aligned}\dot{U}=&2\tilde{\boldsymbol{\theta}}^{\mathrm{T}}\boldsymbol{P}(-k\boldsymbol{L}\tilde{\boldsymbol{\theta}}-\operatorname{diag}\{(\nabla_{\tilde{\boldsymbol{r}}_i}\tilde{V}_i)_\perp\}|\boldsymbol{L}\tilde{\boldsymbol{\theta}}|-\boldsymbol{H}\tilde{\boldsymbol{\theta}})+\\ &2\tilde{\boldsymbol{v}}^{\mathrm{T}}\boldsymbol{P}\left(-k\boldsymbol{L}\boldsymbol{v}-\operatorname{diag}\{(\nabla_{\tilde{\boldsymbol{r}}_i}V_i)_\parallel\}\boldsymbol{L}\tilde{\boldsymbol{v}}-\frac{1}{2}\nabla\tilde{V}-\boldsymbol{H}\tilde{\boldsymbol{v}}\right)+\\ &\sum_{i=1}^{N}\tilde{\boldsymbol{v}}_i^{\mathrm{T}}p_i\sum_{j\in N_i(t)\cup\{l\}}\nabla_{\tilde{\boldsymbol{r}}_i}\tilde{V}_{ij}\leqslant\\ &-\tilde{\boldsymbol{\theta}}^{\mathrm{T}}(k\boldsymbol{Q}+2\boldsymbol{P}\boldsymbol{H})\tilde{\boldsymbol{\theta}}+2f_{\max}||\tilde{\boldsymbol{\theta}}||||\boldsymbol{P}||||\boldsymbol{L}\tilde{\boldsymbol{\theta}}||-\\ &\tilde{\boldsymbol{v}}^{\mathrm{T}}(k\boldsymbol{Q}+2\boldsymbol{P}\boldsymbol{H})\tilde{\boldsymbol{v}}+2f_{\max}||\tilde{\boldsymbol{v}}||||\boldsymbol{P}||||\boldsymbol{L}\tilde{\boldsymbol{v}}||\leqslant\\ &-(\lambda_{\min}(\boldsymbol{\varXi})-2f_{\max}N(N-1))||\tilde{\boldsymbol{\theta}}||^2-\\ &(\lambda_{\min}(\boldsymbol{\varXi})-2f_{\max}N(N-1))||\tilde{\boldsymbol{v}}||^2\end{aligned} \quad (18)$$

where $\boldsymbol{\varXi}=k\boldsymbol{Q}+2\boldsymbol{P}\boldsymbol{H}$, and

$$\operatorname{diag}\{(\nabla_{\tilde{\boldsymbol{r}}_i}V_i)_\parallel\}=\begin{bmatrix}(\nabla_{\tilde{\boldsymbol{r}}_1}\tilde{V}_1)_\parallel & \cdots & 0\\ \vdots & \ddots & \vdots\\ 0 & \cdots & (\nabla_{\tilde{\boldsymbol{r}}_N}\tilde{V}_N)_\parallel\end{bmatrix}$$

$$\operatorname{diag}\{(\nabla_{\tilde{\boldsymbol{r}}_i}V_i)_\perp\}=\begin{bmatrix}(\nabla_{\tilde{\boldsymbol{r}}_1}\tilde{V}_1)_\perp & \cdots & 0\\ \vdots & \ddots & \vdots\\ 0 & \cdots & (\nabla_{\tilde{\boldsymbol{r}}_N}\tilde{V}_N)_\perp\end{bmatrix}.$$

Since $\boldsymbol{P}\boldsymbol{H}$ is positively semi-definite, from Lemma 2 and (16), we can get

$$\dot{U}(t)\leqslant 0,\quad \forall t\in[t_{k-1},t_k);\quad k=1,2,\dots \quad (19)$$

which implies

$$U(t_k)\leqslant U(t_{k-1})<U_{\max},\quad k=1,2,\dots \quad (20)$$

where

$$\begin{aligned}U_{\max}=&\tilde{\boldsymbol{\theta}}^{\mathrm{T}}(0)\boldsymbol{P}\tilde{\boldsymbol{\theta}}(0)+\tilde{\boldsymbol{v}}^{\mathrm{T}}(0)\boldsymbol{P}\tilde{\boldsymbol{v}}(0)+\\ &(N^2-N-1)V_{\max}.\end{aligned} \quad (21)$$

Therefore, for each robot i, no edge distance will tend to R_j $(\forall j\in N_i(t))$ for all $t\in[t_{k-1},t_k)$, which indicates that no edge will be lost at time t_k. Since $G(0)$ is strongly connected and no edges in $E(0)$ will be lost, $G(t)$ is strongly connected for all $t\geqslant 0$.

Similar to the proof of Theorem 1, the set

$$\varOmega=\{\tilde{\boldsymbol{v}}\in\mathbf{R}^{2N},\tilde{\boldsymbol{\theta}}\in\mathbf{R}^N,\tilde{\boldsymbol{r}}\in D_g|U(\tilde{\boldsymbol{v}},\tilde{\boldsymbol{\theta}},\tilde{\boldsymbol{r}})\leqslant U(0)\} \quad (22)$$

is compact, where $D_g=\{\tilde{\boldsymbol{r}}\in\mathbf{R}^{2N^2}|[\min\{V_{ij}^{-1}(U_{\max})\},\max\{V_{ij}^{-1}(U_{\max})\}],\forall(i,j)\in E(t)\}$.

Then it follows the LaSalle's invariance principle that all the trajectories will converge to the largest invariant set inside the set

$$S=\{\tilde{\boldsymbol{v}}\in\mathbf{R}^{2N},\tilde{\boldsymbol{\theta}}\in\mathbf{R}^N,\tilde{\boldsymbol{r}}\in D_g|\dot{U}=0\}$$

which implies $\tilde{\boldsymbol{v}}_1=\tilde{\boldsymbol{v}}_2=\cdots=\tilde{\boldsymbol{v}}_N$ and $\tilde{\theta}_1=\cdots=\tilde{\theta}_N=0$ from (18), i.e., $\boldsymbol{v}_1=\cdots=\boldsymbol{v}_N=\boldsymbol{v}_l$ and $\theta_1=\cdots=\theta_N=\theta_l$. This also implies that in the steady state, $\dot{\theta}_1=\cdots=\dot{\theta}_N=\dot{\theta}_l=0$ and $\dot{\boldsymbol{v}}_1=\cdots=\dot{\boldsymbol{v}}_N=\dot{\boldsymbol{v}}_l=\boldsymbol{0}$. From (15), we have

$$\dot{\boldsymbol{v}}=-\begin{bmatrix}\sum\limits_{j\in N_1\cup\{l\}}\nabla_{\tilde{\boldsymbol{r}}_1}\tilde{V}_{1j}\\ \sum\limits_{j\in N_2\cup\{l\}}\nabla_{\tilde{\boldsymbol{r}}_2}\tilde{V}_{1j}\\ \vdots\\ \sum\limits_{j\in N_N\cup\{l\}}\nabla_{\tilde{\boldsymbol{r}}_N}\tilde{V}_{1j}\end{bmatrix}=\boldsymbol{0}. \quad (23)$$

Thus, almost every final configuration locally minimises each robot's global potential $\nabla_{\tilde{\boldsymbol{r}}_i}\tilde{V}_{ij}$. Finally, following the same procedure in Theorem 1, the collision avoidance between each pair of robots can be proved. □

4. Simulations and experiments

4.1 Simulation of flocking without virtual leader

In this section, comparative numerical simulations are performed to verify the advantage of our connectivity-preserving distributed flocking algorithm with connectivity maintenance over that without connectivity maintenance. The simulations are performed with five agents with dynamics (1) moving in the plane. The number of robots in the group is kept small for clarity of presentation. It is assumed that the initial time $t_0=0$ s, the sensing radii of all the wheeled mobile robots are set to be $R_1 = R_2 = R_4 = 2.5$ m, $R_3 = R_5 = 3$ m. Initial positions, velocities and headings are randomly set, satisfying the following conditions:

(i) All the initial positions of the robots are set within the circle of radius $R = 10$ m with a randomly generated weighted adjacency matrix to meet the requirement that the initial directed communication network is strongly connected.

(ii) All the initial velocities of the robots are chosen randomly with magnitudes belonging to the range of [0, 2 m/s].

(iii) All the initial headings of the robots with arbitrary directions are chosen within $(-\pi, \pi]$.

Furthermore, the potential function V is defined in (5) with the desired distance $d = 2$ m, and $\varepsilon_0 = \varepsilon_2 = 0.2, \varepsilon_1 = 0.5$. The weights are set as $a_{ij} = 1$ for all $(i, j) \in E$. The control gain is set to $k = 10$. Through some simple derivations, we have $V_{\max} = V(R_{\max} - \varepsilon_2)$, then

$$H_{\max} \leqslant N(N-1)V(R_{\max} - \varepsilon_2) + N\lambda_{\max}(\boldsymbol{P}) \max_{i \in V} \tilde{\boldsymbol{v}}_i(0)^{\mathrm{T}} \tilde{\boldsymbol{v}}_i(0) + N\lambda_{\max}(\boldsymbol{P}) \max_{i \in V} \tilde{\theta}_i(0)^{\mathrm{T}} \tilde{\theta}_i(0). \tag{24}$$

Thus we can get $H_{\max} \leqslant 748.3$. Choose $c_1 = c_2 = 50$, we have the explicit form of the potential function.

$$V_{ij}(||\boldsymbol{r}_{ij}||) = \frac{(||\boldsymbol{r}_{ij}|| - 2)^2 (R_j - ||\boldsymbol{r}_{ij}||)}{||\boldsymbol{r}_{ij}|| + \dfrac{(R_j - ||\boldsymbol{r}_{ij}||)}{200}} + \frac{||\boldsymbol{r}_{ij}||(||\boldsymbol{r}_{ij}|| - 2)^2}{(R_j - ||\boldsymbol{r}_{ij}||) + \dfrac{||\boldsymbol{r}_{ij}||(R_j - 2)^2}{800}} \tag{25}$$

Fig. 1 shows the common initial strongly connected but not balanced communication topology for both algorithms. The robots are denoted as red rectangles, the unidirectional neighboring relations between the robots are represented by black solid lines with arrows, and the bidirectional neighboring relations are represented by black solid lines without arrows. The motion trajectories of all robots under the control protocol (4) are depicted in Fig. 2(a) and Fig. 2(b) at $t = 20$ s and $t = 40$ s, respectively, from which it can be seen that all the existing links are kept and the new links are added to the original network as the system evolves, then the strong connectedness of the underlying directed network is preserved. Fig. 2(c) shows that all the robots eventually achieve the same velocities and orientations, while achieving collision avoidance with the neighboring robots during the whole control process. The stable flocking behavior is generated asymptotically.

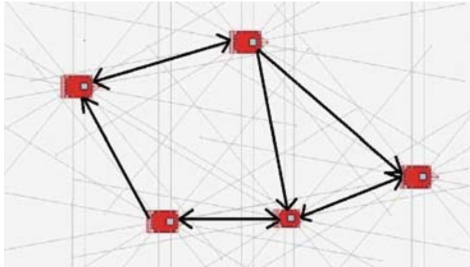

Fig. 1 Initial configuration of five mobile robots

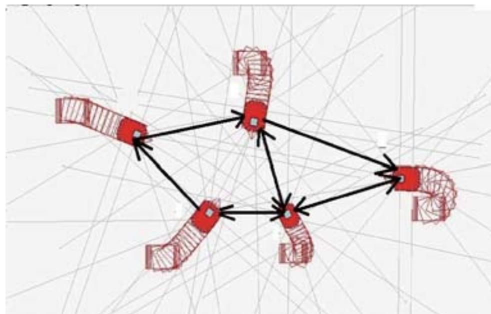

(a) $t = 20$ s

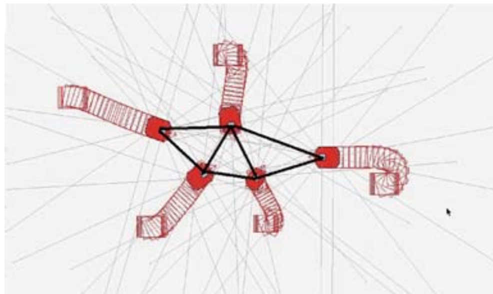

(a) $t = 30$ s

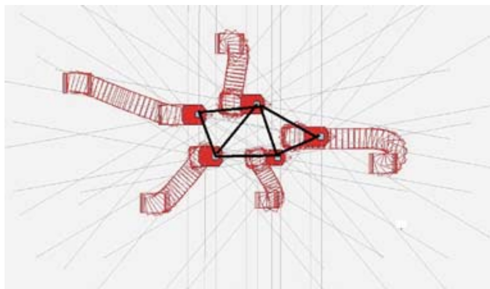

(c) $t = 50$ s

Fig. 2 Flocking of five mobile robots with (4)

Fig. 3(a) and Fig. 3(b) illustrate the synchronization of the velocities along both x and y axes, and the synchronization of the orientations of the group is shown in Fig. 3(c), which verifies the theoretical analysis very well.

The simulation results without connectivity preservation are illustrated in Fig. 4, which shows the typical consecutive video snaps during the whole process of system evolution. It can be concluded that, for some special initial states, the flocking algorithm without connectivity maintenance results in the network fragmentation and the robots finally form different separated subgroups instead of forming a cohesive connected flock. The velocities and orientations of all robots fail to synchronize to a common value as a whole. On the contrary, the stable group flocking behavior could be achieved under control protocal (4) by utilizing the bounded artificial potential functions (5). Therefore, the conclusion can be safely drawn that the connectivity preservation is indispensable and the potential functions with connectivity preserving should be well-designed to ensure the stability of the whole flock under arbitrary initial configurations.

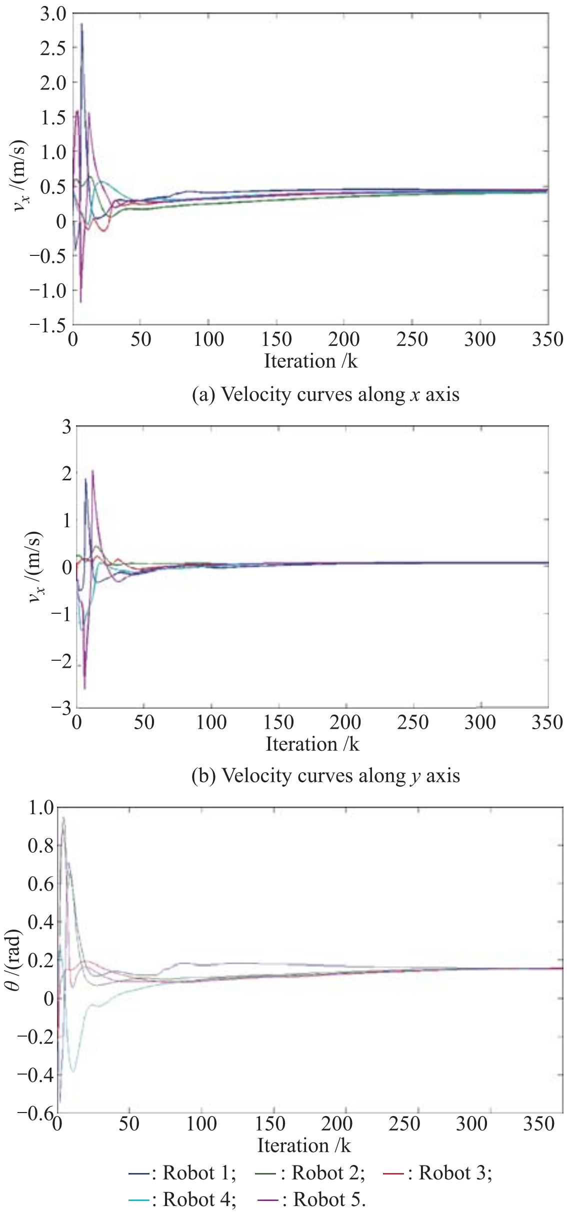

(a) Velocity curves along x axis

(b) Velocity curves along y axis

(c) Orientation curves

Fig. 3 Velocity and orientation curves of five mobile robots

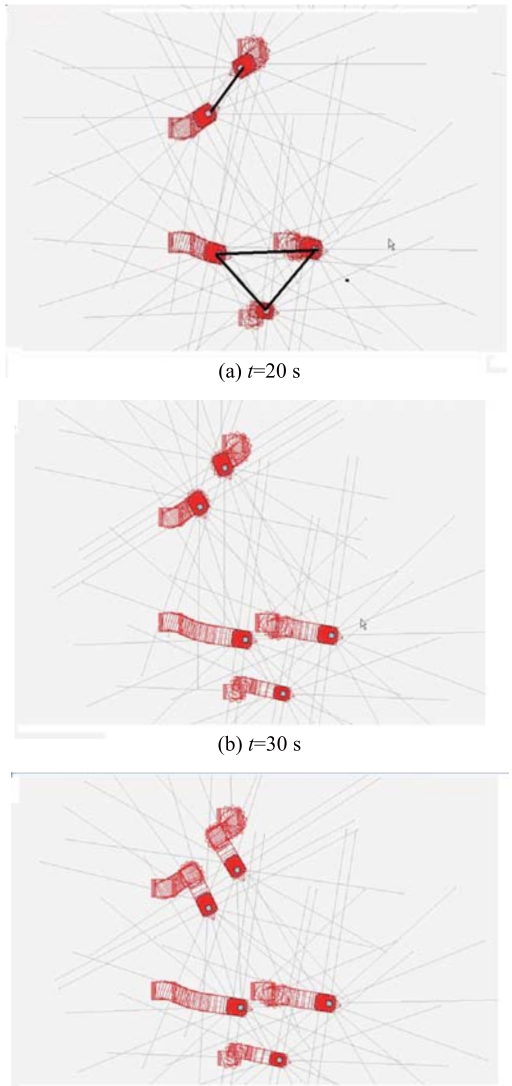

(a) t=20 s

(b) t=30 s

(c) t=40 s

Fig. 4 Simulation of flocking of five mobile robots without connectivity maintenance

4.2 Experiment of flocking without virtual leader

In this section, the experimental results are presented to illustrate the effectiveness of the control protocal (4), which are performed with five differential-drive nonholonomic wheeled mobile robots that consist of four Pioneer3-AT robots and a Pioneer3-DX robot. The initial positions are initialized to ensure that the initial network is strongly connected. The linear velocities of the robots are randomly chosen in the range of [0, 2 m/s], and the maximum speed is 3 m/s. The control period is $T = 0.5$ s and the communication radii are set to $R_1 = R_2 = R_4 = 2.5$ m, $R_3 = R_5 = 3$ m. The desired distance is $d = 1$ m. Moreover, it is assumed that all the robots are subject to nonslipping and pure-rolling constraints and each robot has access to the information needed via its wireless communication equipment.

Fig. 5 illustrates typical experiment snapshots during the entire evolution of the proposed flocking protocal (4). The unidirectional communication links are denoted by the solid yellow lines with red arrows, and the bidirectional communication links are denoted by the solid yellow lines without arrows.

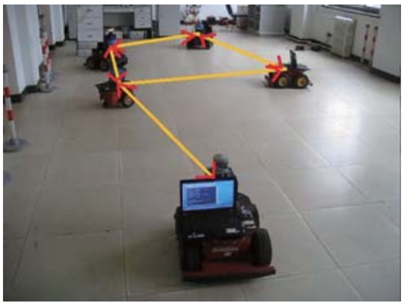

(a) t=0 s

(b) t=20 s

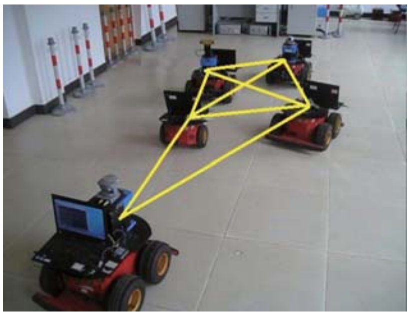

(c) t=35 s

(d) Final state

Fig. 5 Experiment validation of flocking of five mobile robots

Fig. 5(a) shows the initial configuration of the strongly connected directed but not balanced communication topology. Fig. 5(b) and Fig. 5(c) illustrate the consecutive typical snapshots of the motion evolution process at $t = 20$ s and $t = 35$ s. The final state of the system is shown in Fig. 5(d). It is obvious that the strongly connectedness of the underlying time-varying directed network is preserved during the whole system evolution. All the robots could successfully obtain the same velocities and orientations as a cohesive flock without collisions, and the stable desired flocking motion is finally achieved asymptotically.

4.3 Simulation of flocking with virtual leader

Finally, simulations of flocking with a virtual leader under control protocol (15) are performed with five agents moving in the Euclidean plane. The communication radii of all the robots are set as $R_1 = R_5 = 5$ m, and $R_2 = R_3 = R_4 = 3$ m, respectively. Once again, the initial directed network is set to be strongly connected but not balanced. Initial velocities of the five agents are chosen randomly from the range of [–3 m/s, 3 m/s]. The desired velocity and orientation of the virtual leader are chosen as $v_l = 2$ m/s and $\theta_l = -\pi/2$, respectively. The values are set as $\varepsilon_1 = 0.9$, $\varepsilon_0 = \varepsilon_2 = 0.5$. It can be easily deduced that $V_{\max} = V(R_{\max} - \varepsilon_2)$ and according to (5), we have

$$\begin{aligned} H_{\max} \leqslant\ & N(N-1)V(R_{\max} - \varepsilon_2) + \\ & N\lambda_{\max}(\boldsymbol{P}) \max_{i\in V} \tilde{\boldsymbol{v}}_i^{\mathrm{T}}(0)\tilde{\boldsymbol{v}}_i(0) + \\ & N\lambda_{\max}(\boldsymbol{P}) \max_{i\in V} \tilde{\boldsymbol{\theta}}_i^{\mathrm{T}}(0)\tilde{\boldsymbol{\theta}}_i(0). \end{aligned} \tag{26}$$

Thus we get $H_{\max} \leqslant 1\,990.7$, further choose $c_1 = c_2 = 10, d = 2$, then the bounded potential function (5) is selected as follows:

$$\begin{aligned} V_{ij}(||\boldsymbol{r}_{ij}||) = & \frac{(||\boldsymbol{r}_{ij}|| - 2)^2(R_j - ||\boldsymbol{r}_{ij}||)}{||\boldsymbol{r}_{ij}|| + \dfrac{(R_j - ||\boldsymbol{r}_{ij}||)}{500}} + \\ & \frac{||\boldsymbol{r}_{ij}||(||\boldsymbol{r}_{ij}|| - 2)^2}{(R_j - ||\boldsymbol{r}_{ij}||) + \dfrac{||\boldsymbol{r}_{ij}||(R_j - 2)^2}{2000}}. \end{aligned} \tag{27}$$

Fig. 6 shows the whole process of the simulation with a period of 50 s. Fig. 6(a) depicts the initial state of the system, in which the informed agent is chosen randomly from the group and marked with a capital letter '$\boldsymbol{L}$'. Fig. 6(b) and Fig. 6(c) illustrate the consecutive video snaps at $t = 10$ s and $t = 30$ s. It is obvious that the initially dispersed robots tend to form a cohesive flock without violating the strong connectedness of the network. The final state is shown in Fig. 6 (d), from which it can be seen that the velocities and headings of all robots finally become the same and the stable flocking motion is asymptotically achieved without collisions.

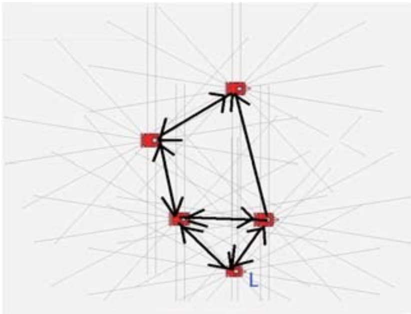

(a) Initial state

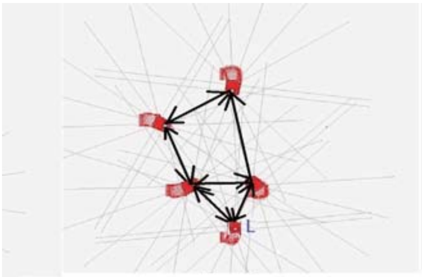

(b) t=10 s

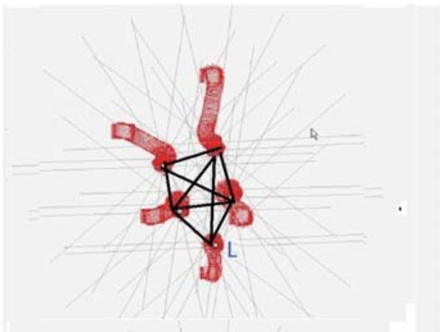

(c) t=30 s

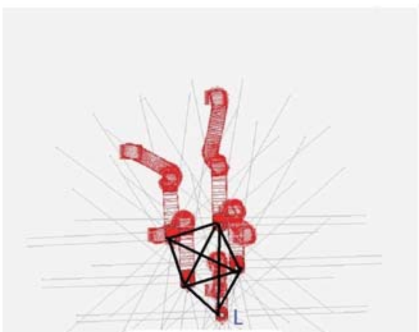

(d) Final state

Fig. 6 Flocking of five mobile robots with (15)

Fig. 7 demonstrates the tracking results with a virtual leader qualitatively and quantitatively. Fig. 7(a)–Fig. 7(c) show the convergence of and the velocity tracking errors of each robot along the x and y axes orientation tracking errors, respectively, from which it can be observed that all the tracking errors asymptotically converge to zero. Therefore, all agents eventually reach the desired velocity $\boldsymbol{v}_l$ and the desired orientation θ_l.

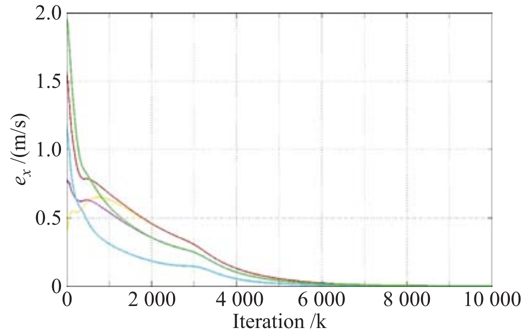

(a) Velocity tracking errors along x axis

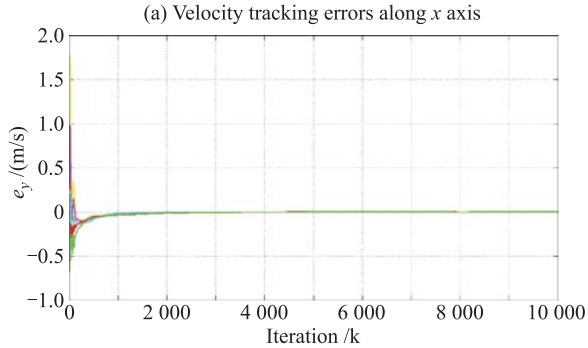

(b) Velocity tracking errors along y axis

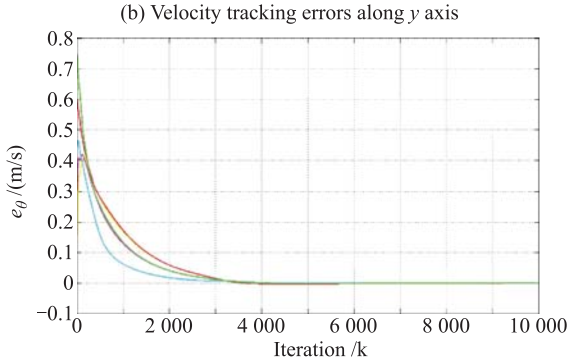

(c) Orientation tracking errors

—: Error 1; —: Error 2; —: Error 3; —: Error 4; —: Error 5.

Fig. 7 Velocity and orientation convergence of five mobile robots

5. Conclusions and future work

In this paper, a set of distributed flocking algorithms with bounded control inputs has been investigated to enable the multi-robot systems with nonholonomic kinematics. Through devising a new class of bounded artificial potential functions which nicely integrates the collision avoidance, inter-distance stabilization and connectivity maintenance simultaneously, all the existing communication links are preserved, the velocities and orientations of all robots are guaranteed to be synchronized, and collisions between the robots are avoided. It has been shown that the proposed algorithm could enable the group of multiple robots to asymptotically achieve the stable flocking motion, provided that the initial directed network is strongly connected but not balanced and the algebraic connectivity of its augmented weighted mirror graph is larger than a threshold. Moreover, the problem of cooperative flocking with a virtual leader has also been investigated. With the modified local control protocols, all the robots could achieve velocity and orientation synchronization as well as collision avoidance even if only one robot has the information about the virtual leader. Finally, extensive simulations and experiments have been performed, which showes the consistency with the theoretical results.

However, there are some issues that need to be addressed in the future. First, it will be interesting and challenging to derive flocking control protocols by using only position information. Second, it will be also interesting to extend the proposed bounded flocking control strategies to more complex environmental settings with multiple moving obstacles and more general directed networks.

References

[1] M. M. Zavlanos, M. B. Egerstedt, G. J. Pappas. Graph-theoretic connectivity control of mobile robot networks. *Proceedings of the IEEE*, 2011, 99(9): 1525–1540.

[2] C. W. Reynolds. Flocks, herds, and schools: a distributed behavioural model. *Computer Graphics*, 1987, 21(6): 25–34.

[3] T. Vicsek, A. Czirook, E. Ben-Jacob, et al. Novel type of phase transition in a system of self-deriven particles. *Physcial Review Letters*, 1995, 75(8): 1226–1229.

[4] H. G. Tanner, A. Jadbabaie, G. J. Pappas. Flocking in fixed and switching networks. *IEEE Trans. on Automatic Control*, 2007, 52(5): 863–868.

[5] R. Olfati-Saber, R. M. Murray. Flocking with obstacle avoidance: cooperation with limited communication in mobile networks. *Proc. of the 42nd IEEE Conference on Decision and Control*, 2003: 2022–2028.

[6] A. Jadbabaie, J. Lin, A. S. Morse. Coordination of groups of mobile agents using nearest neighbor rules. *IEEE Trans. on Automatic Control*, 2003, 48(6): 988–1001.

[7] R. Olfati-Saber. Agreement problems in networks with directed graphs and switching topology. *Proc. of the 42nd IEEE Conference on Decision and Control*, 2003: 4126–4132.

[8] R. Olfati-Saber. Flocking for multi-agent dynamic systems: algorithms and theory. *IEEE Trans. on Automatic Control*, 2006, 51(3): 401–420.

[9] Z. Y. Wang, D. B. Gu. Distributed leader-follower flocking control. *Asian Journal of Control*, 2009, 11(4): 396–406.

[10] H. S. Su, X. F. Wang, W. Yang. Flocking in multi-agent systems with multiple virtual leaders. *Asian Journal of Control*, 2008, 10(2): 238–245.

[11] R. Murphy, J. Kravitz, S. Stover, et al. Mobile robot in mine rescue and recovery. *IEEE Robotics and Automation Magazine*, 2009, 16(3): 91–103.

[12] H. S. Su, X. F. Wang, G. R. Chen, et al. Adaptive second-order consensus of networked mobile agents with nonlinear dynamics. *Automatica*, 2011, 47(2): 368–375.

[13] R. Olfati-Saber, J. Fax, R. Murray. Consensus and cooperation in networked multi-agent systems. *Proceedings of the IEEE*, 2007, 95(1): 215–233.

[14] Y. Kim, M. Mesbahi. On maximizing the second smallest eigenvalue of a state-dependent graph Laplacian. *IEEE Trans. on Automatic Control*, 2006, 51(1): 116–120.

[15] M. M. Zavlanos, G. J. Pappas. Potential fields for maintaining connectivity of mobile networks. *IEEE Trans. on Robotics*, 2007, 23(4): 812–816.

[16] M. Ji, M. Egerstedt. Distributed formation control while preserving connectedness. *Proc. of the 45th IEEE Conference on Decision and Control*, 2006: 5962–5967.

[17] M. Ji, M. Egerstedt. Distributed coordination control of multi-agent systems while preserving connectedness. *IEEE Trans. on Robotics*, 2007, 23(4): 693–703.

[18] M. M. Zavlanos, G. J. Pappas. Flocking while preserving network connectivity. *Proc. of the 46th IEEE Conference on Decision and Control*, 2007: 2919–2924.

[19] X. L. Li, Y. G. Xi. Distributed cooperative coverage and connectivity maintenance for mobile sensing devices. *Proc. of the 48th IEEE Conference on Decision and Control*, 2009: 7891–7896.

[20] H. S. Su, X. F. Wang, G. R. Chen. Rendezvous of multiple mobile agents with preserved network connectivity. *Systems & Control Letters*, 2010, 59(5): 313–322.

[21] N. Chopra, M. W. Spong. Passivity-based control of multi-agent systems. S. Kawamura, M. Svinim. *Advances in robot control: from everyday physics to humanlike movements*. Berlin, Germany: Springer, 2006.

[22] W. W. Yu, G. R. Chen, M. Cao, et al. Second-order consensus for multiagent systems with directed topologies and nonlinear dynamics. *IEEE Trans. on Systems, Man, and Cybernetics — Part B: Cybernetics*, 2010, 40(3): 881–891.

[23] D. V. Dimarogonas, K. J. Kyriakopoulos. Connectivity preserving distributed swarm aggregation for multiple kinematic robots. *IEEE Trans. on Robotics*, 2008, 24(5): 1213–1223.

[24] W. Ren. Synchronization of coupled harmonic oscillators with local interaction. *Automatica*, 2008, 44(12): 3195–3200.

[25] L. Wang, X. F. Wang. Flocking of mobile agents while preserving connectivity based on finite potential functions. *Proc. of the 8th IEEE International Conference on Control and Automation*, 2010: 2056–2061.

[26] I. D. Couzin, J. Krause, N. R. Franks, et al. Effective leadership and decision-making in animal groups on the move. *Nature*, 2005, 433(2): 513–516.

[27] K. Savla, G. Notsrstefano, F. Bullo. Maintaining limited-range connectivity among second-order agents. *SIAM Journal on Control and Optimization*, 2009, 15(5): 187–205.

[28] H. S. Su, X. F. Wang, G. R. Chen. A connectivity-preserving flocking algorithm for multi-agent systems based only on position measurements. *International Journal of Control*, 2009, 82(7): 1334–1343.

[29] D. P. Spanos, R. M. Murray. Robust connectivity of networked vehicles. *Proc. of the 42nd IEEE Conference on Decision and Control*, 2004: 2893–2899.

[30] K. Savla, G. Notsrstefano, F. Bullo. Maintaining limited-range connectivity among second-order agents. *SIAM Journal on Control and Optimization*, 2009, 15(5): 187–205.

[31] J. Cortes, S. Martinez, F. Bullo. Robust rendezvous for mobile autonomous agents via proximity graphs in arbitrary dimensions. *IEEE Trans. on Automatic Control*, 2006, 51(8): 1289–1298.

[32] M. C. DeGennaro, A. Jadbabaie. Decentralized control of connectivity for multiagent systems. *Proc. of the 45th IEEE Conference on Decision and Control*, 2006: 3628–3633.

[33] P. Yang, R. A. Freeman, G. J. Gordon, et al. Decentralized estimation and control of graph connectivity for mobile sensor networks. *Automatica*, 2010, 46(2): 390–396.

[34] M. M. Zavlanos, H. G. Tanner, A. Jadbabaie, et al. Hybrid control for connectivity preserving flocking. *IEEE Trans. on Automatic Control*, 2009, 54(12): 2869–2875.

[35] M. M. Zavlanos, G. J. Pappas. Distributed connectivity control of mobile networks. *IEEE Trans. on Robotics*, 2008, 24(6): 1–12.

[36] N. Li, J. C. Hou, L. Sha. Design and analysis of an MST-based topology control algorithm. *IEEE Trans. on Wireless Communications*, 2005, 4(3): 1195–1206.

[37] L. Sabattini, N. Chopra, C. Secchi. On decentralized connectivity maintenance for mobile robotic systems. *Proc. of the 50th IEEE Conference on Decision and Control*, 2011: 1651–1655.
[38] L. Sabattini, C. Secchi, N. Chopra. Decentralized connectivity maintenance for networked lagrangian dynamical systems. *Proc. of the IEEE International Conference on Robotics and Automation*, 2012: 2433–2438.
[39] C. Secchi, L. Sabattini, C. Fantuzzi. Decentralized global connectivity maintenance for interconnected Lagrangian systems in the presence of data corruption. *European Journal of Control,* 2013, 19(2): 461–468.
[40] D. V. Dimarogonas, K. J. Kyriakopoulos. On the rendezvous problem for multiple nonholonomic agents. *IEEE Trans. on Automatic Control*, 2007, 52(5): 916–922.
[41] D. V. Dimarogonas, K. H. Johansson. Bounded control of network connectivity in multi-agent systems. *IET Control Theory & Applications*, 2010, 4(8): 1330–1338.
[42] A. Ajorlou, A. Momeni, A. G. Aghdam. A class of bounded distributed control strategies of connectivity preservation in multi-agent systems. *IEEE Trans. on Automatic Control*, 2010, 55(12): 2828–2832.
[43] C. Godsil, G. Royle. *Algebraic graph theory*. Berlin: Springer, 2001.
[44] Z. H. Qu. *Cooperative control of dynamical systems: applications to autonomous vehicles*. London: Springer, 2009.
[45] R. A. Horn, C. Johnson. *Matrix analysis*. Cambridge: Cambridge University Press, 1985.
[46] H. K. Khalil. *Nonlinear systems*. 3rd ed. New Jersey: Prentice-Hall, 2002.

Biographies

Yutian Mao was born in 1984. He is a Ph.D. candidate at School of Automation, Beijing Institute of Technology. His research interest covers distributed motion coordination and cooperation of networked multi-robot systems.
E-mail: virtual123@126.com

Lihua Dou was born in 1961. She is a professor at School of Automation, Beijing Institute of Technology. Her main research interests include multi-robot coordination, intelligent control, and expert system.
E-mail: doulihua@bit.edu.cn

Hao Fang was born in 1973. He is a professor at School of Automation, Beijing Institute of Technology. His main research interests include multi-agent formation control, robotic control and parallel manipulator.
E-mail: fangh@bit.edu.cn

Jie Chen was born in 1965. He is a professor at School of Automation, Beijing Institute of Technology. His research interest covers complex system multi-objective optimization and decision, constrained nonlinear control, and optimization methods.
E-mail: chenjie@bit.edu.cn